Biomedical & Pharmacology Journal, March 2026. Vol. **19**(1), p. 694-718

Design a Low Cost Device for Preventing Fetal Distress by Analysis of Heart Rate

Nguetsop Hermann Beaumont[1]*, Jean Mbihi[1], Gamom Ngounou[1] and Moffo Lonla[2]

[1]Department of Computer Science Engineering Automation and Bioengeneering of HTTTC, University of Douala, Douala, Cameroon.
[2]Department of Health Sciences of HTTTC, University of Ebolowa, South, Cameroon.
*Corresponding Author E-mail: beaumont.nguetsop@yahoo.com

https://dx.doi.org/10.13005/bpj/3386

(Received: 10 October 2025; accepted: 15 December 2025)

This article describes the design of a device for analyzing and extracting parameters from pregnant women. This is achieved primarily by isolating fetal and maternal cardiac signals. The objective is to contribute to addressing the problem of rising intrauterine fetal mortality in the most isolated regions of developing countries: the case of Cameroon. Our case study focuses on a problem observed in low-income countries: the difficulty of accessing regular medical care for many pregnant women due to the unavailability of doctors and the lack of equipment in health centers. The design and use of less expensive remote fetal monitoring devices is therefore an essential solution. Our technique is based on the preprocessing of signals modulating the maternal ECG (ECG-M) and the fetal ECG (ECG-F), acquired using the DCM (cycle-ratio modulation) method with ultrasound Doppler probes. The composite signal is then separated by a SOBI (second-order blind identification) algorithm. Filtering performed using a filter derived from the Pan-Thomkins structure for detecting ECG R peaks and a heart rate calculation algorithm. The simulation performed using Matlab-Simulink software (2020b). To verify the real-time operation of our cardiac system, we used the FECGSYNDB database (fetal electrocardiogram synthetic database) on an ESP32 board for simulation evaluation of the fetal ECG extraction algorithms, and 30 volunteer patients for practical validation of our device. Finally, the resulting device used for real-time recording in numerous hospitalized patients, and the results were compared to those of existing wearable devices reviewed. Our results demonstrate relatively good performance considering its cost of USD 66. With a separability index of 0.0011 and a 20-hour battery life with a 2500 mAh battery, it detects 97% of the R peaks of physiological cardiac signals. This performance, while satisfactory for us, is superior to that reported by several authors in the literature: accuracy (99.01%), sensitivity (97.45%), specificity (97.09%), precision (98.11%), and F1 score (96.89%). Regarding fetal arrhythmia, our model presents the following results: sensitivity (FECG) = 98.96%; fetal precision (P+FECG) = 99.01%; F1 score (FECG) = 99.51 ± 0.14%. It informs the pregnant woman at any time whether her fetal heart rate is normal, requires monitoring, or is abnormal, facilitating prompt medical intervention.

Keywords: Blind source separation; Battement per Minutes; Cardiac Arrhythmias; Duty Cycle Modulation; Doppler ultrasonic; ESP 32 WROOM; FECGSYNDB; Fetal ECG; Fœtal Heart Rate; Internet of Things; Maternal ECG; Second Oder Blind Identification.

Stillbirth or fetal death is a term used by the WHO (World Health Organization) [1] when the death of a fetus occurs in the mother's womb. The data collected in different hospital facilities in the West show that the intrauterine mortality rate oscillates between 8.5 and 9 cases per 1000

births between [2014 and 2021] (Europerisat). Its figures are alarming because it shows that cardiovascular abnormalities represent the most frequent cause of these deaths. As the fetal heart muscle is still in its preliminary state of growth, perinatal death may be noted by the doctor several days later, thus endangering the mother's life. UNICEF and the WHO have set new targets to end preventable newborn deaths and stillbirths and accelerate the achievement of quality universal health coverage by 2020- 2025 (September 2020)[2] with future consequences of at least four antenatal consultations for every pregnant woman in the world. This solution faces many problems, including insufficient financial resources to equip all health centers with adequate equipment in order to meet all targets. Several scientific works have gegun to resolve this difficulty by early diagnosis of cardiac arrhythmias; which has encouraged the development of numerous fetal remote monitoring devices. However, the presence of the mother in a hospital center remains obligatory. Remote monitoring is therefore essential as a solution. Progress in medical bioinstrumentation has enabled the birth of several mobile devices whose reliability remains to be perfected. The previously cited figures remain enormous in contrast to the wealth of the technical platform of hospitals outside the African continent. Unfortunately, despite the efforts undertaken with the help of development partners, the expected results were not obtained. Indeed, the maternal mortality ratio deteriorated from 500 to 800 deaths per 100,000 live births between 2010 and 2020. In Cameroon, this figure is poorly estimated due to the difficult access of pregnant women to constant medical monitoring, the insufficiency of technical platforms, the low standard of living of women, the insufficiency of qualified doctors especially in rural areas or there is probably one doctor for more than 20,000 inhabitants. Seen from this angle, this figure would be at least quadruple that of Western countries. How can we create a low-cost portable device capable of extracting and processing fetal heart signals FECG and informing the patient of the permanent state of health of her fétus? In this case, if the patient experiences brief and recurring discomfort, a portable FECG signal recorder is made available to her, allowing her to record arrhythmias at home and encourage rapid treatment by doctors. Direct use of intrauterine electrocardiographic probes on the fetyal head is an inaccurate and dangerous method.

To resolve this problem, methods of extracting fetal parameters without contact were born, in particular the use of ultrasound probes by Doppler Effect. Whereas in a signal extracted with Doppler probes, [3] these processes are seen as a difference between the wave emitted by the probe and the wave incident on the fetal heart walls. The frequency of the beats and the amplitude are the only differences between the cardiac signals of adults and those of fetuses, particularly drowned out in several other sources of noise (skin ; intestines, blood circulation, amniotic fluid of the mother) wemust necessarily isolate the useful signal from everything else. A fist partial solution for BSS (Blind Sources Separation) [4] was foubd by scientifics to solve this, using ICA (Independent Component Analysis) [5, 6, 7] is the main vector of non-adaptive diffusion of ECG signal extraction method. During ICA (independent analysis of components) preprocessing, centering is applied. We then whiten, thus creating a new vector with uncorrelated components and unit variances. [8,9,10] Many studies have been done in the past for BSS (blind source separation)[11,12] using neural networks and FPGA (Field Programmable Gate Area) hardware (of all brands and characteristics),[13] and proposed a less expensive FPGA hardware architecture based on an algorithm ICA (independent component analysis) to perform fetal cardiac signal extraction from the maternal one. Some of them have instead used several methods combining EMD (empirical mode decomposition),[14] FIR filtering (Filter Impulse Response) and (ICA).[15] The characteristics based on statistics and entropy have been used at several levels in order to evaluate the quality of ECG signals. Recently some authors have addressed the challenge of real-time source separation using Arduino Due board [16, 17, 18] and ESP 32 WROOM board.[19, 20, 21] However, to date, none of these studies have addressed the challenge of real-time source separation acquired at two different locations using Doppler ultrasonic sensors; modulated by DCM techniques and implemented in a single ESP32 board known to be a low-power and low-cost material. Our application then aims to separate in real time the fetal cardiac activities (FECG) using an HB100 ultrasound probe from those of the mother (MECG) using another JSN-SR04T

ultrasound scale in order to inform the mother of the nature of these beats (normal beats, bradycardia or tachycardia). To achieve our challenge of separating the fetal signal from the maternal signal in real time, we userd improved version of the algoritms and methods developed in the articles.[16, 17] The Matlab/Simulink software for the simulation and the ESP32 card for the implementation. Some innovative strengths of our device:

• The price-performance ratio is affordable for solving the poverty problem associated with patients in low-income countries.

• Comparison with a conventional portable fetal monitoring device shows a 5 percent higher fidelity.

• Our device measures 15 cm x 7 cm, with a continuous battery life of 6 hours.

• The SOBI source separation algorithm used offers significantly better performance than those in the literature review.

• The ultrasound penetration depth in real-life operation is average and ensures the extraction of the AECG signal.

• Our Core 2 ESP 32 card demonstrates an operating flexibility of 20 percent of its total capacity, which minimizes bugs.

The results will be displayed on a 16 x 2 LCD screen. We then divided our work into three main parts: the introduction; material and method; results and discussion and conclusion.

MATERIALS AND METHODS

Type of sampling and reasons for selection

A purposive sampling technique was used for this retrospective study. Patients were selected according to predefined inclusion criteria: pregnant woment volunteers whose signals are recorded in the dataset. Sampling was limited to patients with gestational ages starting at 12 weeks of amenorrhea.

Patient consent statement

This study was conducted as a retrospective analysis using anonymized data extracted from existing medical records. In accordance with IEC guidelines and the Declaration of Helsinki, individual patient consent was not required, as no personally identifiable information was collected or shared. All data were treated with the strictest confidentiality, and patient privacy was rigorously protected throughout the research process.

Exclusion criteria

Patients excluded were minors under 21 years of age and those whose gestational age was less than 12 weeks of ammenorrhea.

Consentement to publication

Not applicable. This manuscript adheres to the STROBE guidelines for observational computational research."

To solve our problem which is to create a portable device at a lower cost capable of extracting and processing fetal heart signals FECG and informing the patient of the permanent state of health of her fetus, we use severals materials and software.

Materials

The JSN-SR04T Ultrasonic Sensor

JSN-SR04T-2.0 (*Figure.1.A*) is non-contact distance sensing.[39] Operating Voltage = DC [3.0 – 5.5] V. Probe frequency = Less than 400 KHz.It is send beetween 5.5 and 7 €. Placed on the mother's rib cage, this probe will measure the frequency of the mother's heartbeat using its Doppler echo. Indeed, with each pulse, the volume of blood in the heart muscle increases and therefore its size; which also decreases with each release. The sensor returns the incident wave and thanks to it, the heart rate per minute can be calculated. The latter works in pulsed Doppler which will be developed in the method section, the ultrasonic timing diagram [49] show as (*Figure.1.C)*.

The HB 100 Ultrasonic Sensor

Ultrasonic Doppler Detection Sensor (Figure. 1 B) with a maximum frequency of 10.525 GHz.[30] Placed on the mother's lower abdomen using a mobile belt around the waist, this probe will measure the fetal heart rate using its incident Doppler echo. It is sold for between 5 and 7 €.

THE Duty-Cycle Modulation (DCM) Diagramm

Indeed, with each pulse, the volume of blood in the heart muscle increases and therefore its size and decreases with each relaxation. The sensor returns the incident wave and thanks to it, the heart rate per minute can be calculated. The latter works in continuous Doppler which will be developed in the method section.[45]

The output signal must be amplified before being used, this is why a conditioner assembly is necessary and the diagram is that of (*Figure.1 C*). A Duty-Cycle Modulation (DCM) with the analog filter, Interfacing HB100 diagram for correct use

with ESP 32 then follows it. The waveform taken from the output of the DCM block is as follows (*Figure.1 G*).[45] give the Fourier series expansion of the modulated signal xm (t):

$$x_m(t) = \left(2R_m\left(x(t)\right) - 1\right)E + \sum_{n=1}^{\infty}\left(\left(\frac{4E}{\pi}\right)\frac{\sin(n\pi R_m(x(t)))}{n}.\cos\left(2\pi n\frac{t}{T_{osc}(x(t))}\right)\right) \quad ...(1)$$

And the duty cycle R_m is given by the relation [36]:

$$R_m\left(x(k)\right) = \frac{T_{on}\left(x(k)\right)}{T_m\left(x(k)\right)} = \frac{ln\left(\frac{\alpha_2 x(k) - (1+\alpha_1)}{\alpha_2(x(k))+(\alpha_1-1)E}\right)}{ln\left(\frac{(\alpha_2 x(k))^2-((1+\alpha_1)E)^2}{(\alpha_2 x(k))^2-((\alpha_1-1)E)^2}\right)} \quad ...(2)$$

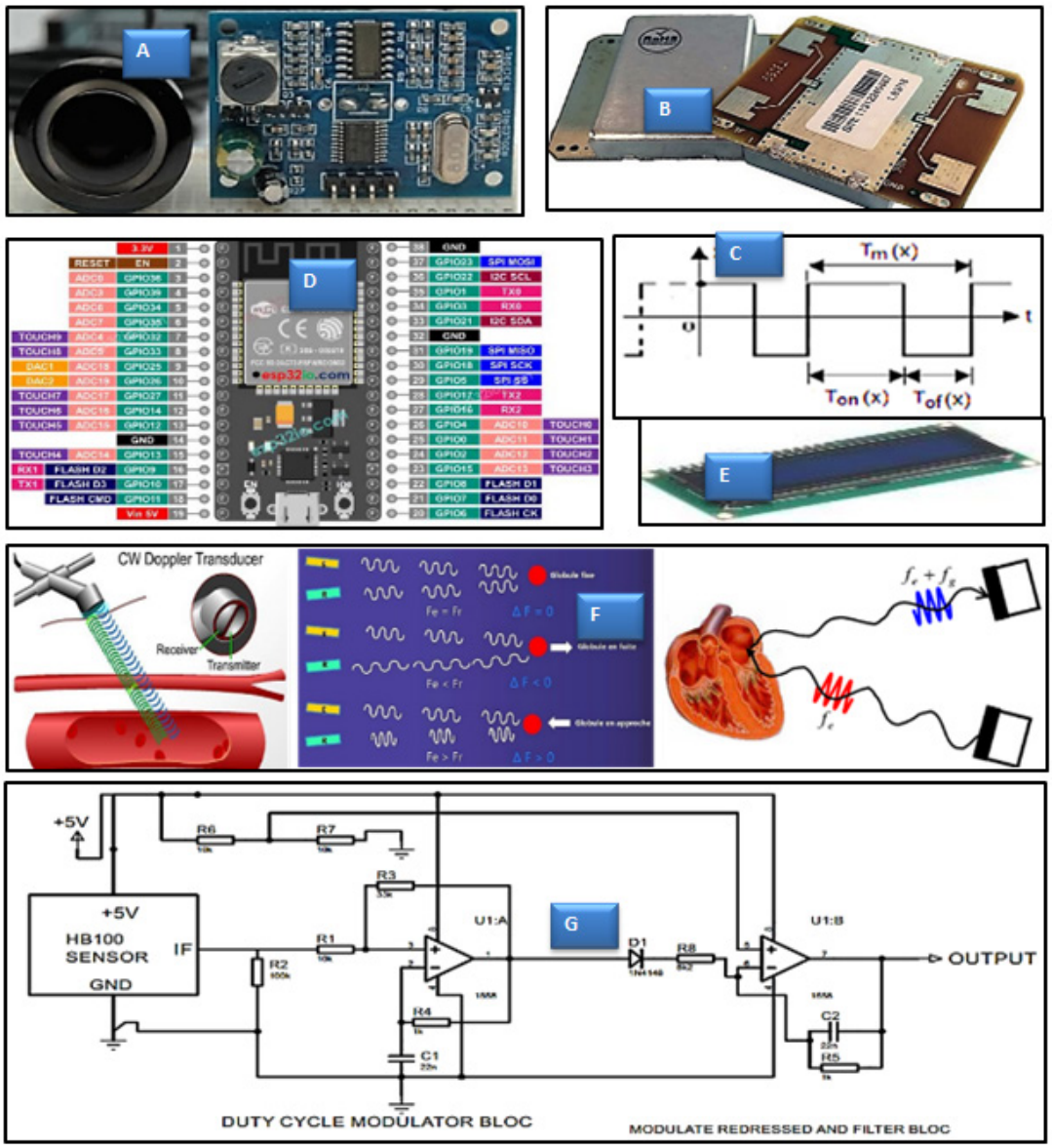

Fig.1. A (Physical presentation Doppler ultrasonic sensor JSN-S04T). B (Physical presentation Doppler ultrasonic sensor HB 100)[39]. C (explanatory figure of the waveform and duty cycle of our DCM). [36] D. (Psysical presentation of ESP and GPIO configuration). [49] E (LCD I2C display 16x2). F. (Emission, displacement and refraction of ultrasound waves in the blood and the heart: Doppler Effect).

α1 and α2 = 1 - α1 are parameters of the modulator. By substituting α2 = 1 - α1 into (2), R(x) will exhibit a linearity that is optimal for (α1 ≤ 0.2)[36].

The ESP 32 wroom board.

Psysical presentation of ESP and GPIO Configuration *(*Figure.1 G*).* [49] The technical performances, electrical characteristics and other parameters that justified the choice of our ESP card among several other existing cards are recorded in the table 1.

Display information

We used a 16x2 I2C LCD display to display information after processing (*Figure.1. E*).

Methods

The proposed technique in complète organigram of our device (*Figure.2.A*). Is based on the processing of signals modulating MECG and FECG acquired by Duty Cycle Modulation (DCM) using ultrasonic Doppler probes. A modified SOBI algorithm then separates the mixture; a filter deriving from the structure of Pan carries out the filtering and Thomkins for the detection of R peaks of the PQTRS complex of ECGs and the algorithm for calculating the heart rate all its functions are realized and simulated using Matlab-Simulink software (2020b). Implement us in an ESP 32 WROOM card as shown in (*Figure.2.B*). We use FECGSYNDB for confirm our approach, this database have the vital sign of several patients volunteers for practical validation.

Doppler Effect and ultrasound

The Doppler Effect is the shift between the emitted and incident frequencies of a sound wave when the distance between the transmitter and the receiver varies over time.[3] we observe it daily without realizing it. For example, the sound of a car is higher pitched when it is approaching us and lower pitched when it is moving away. A probe emits ultrasound waves at a frequency F_e. These waves propagate in the soft tissues towards the vessel to be explored where they encounter the moving blood column.[28] the movement of the red blood cells causes backscattering of the ultrasound wave.

$$F_d = Fr - Fe = \frac{2\,Fe\,.V.\cos\theta}{C} \quad ...(3)$$

F_d: Difference between frequency of the transmitted wave and that of the received wave.
F_r: Frequency of the reception wave.
F_e: Frequency of the emitted wave.
V: Blood flow velocity.
C: Speed of the US in the medium considered (1540m/s).
Cos è: Cosine angle between incident ultrasound beam and the direction of blood flow.
The blood cell or wall of the heart perceives a frequency Fe.

$$F_e = \left(1 - \frac{V.\cos\theta}{C}\right) \quad ...(4)$$

The signal is then broadcast towards the source which perceives a frequency Fer (assuming that V<<C).

$$F_r = \left(1 + \frac{V.\cos(\pi-\theta)}{C}\right) \quad ...(5)$$

The shift in frequency of the signal broadcast by the heart walls or red blood cells, perceived by the transmitter/receiver is therefore worth ΔF if V<<C.

$$\Delta F = F_r - F_e = \left(\frac{2\,V.\cos\theta}{C}\right) Fe \quad ...(6)$$

The frequency shift is small; we observe by adding the signal received and the signal transmitted, we obtain the heartbeats of frequency "F which we isolate using signal processing. It then reflects the evolution of blood speed during heart rhythms. Emission, displacement and refraction of ultrasound waves in the blood and the heart: Doppler Effect (Figure.1 G)

Continuous doppler (DC)

Two crystals at the same sensor: one emits the other receives continuously.[37] The device makes the difference between Fr and Fe continuously. DC Doppler allows examination of blood flow data and collects samples along the entire beam in mode rather than at a specific location. Advantages: great sensitivity to slow flows; absence of limit for calculating rapid flows. Disadvantages: Blind shooting on the entire trajectory. We use it in HB100.

Pulse doppler

A pulsed ultrasound emission makes it possible to determine the distance of the Doppler echoes and to measure their speed. The speed of the ultrasound wave being approximately constant in

Table 1. Technical Specifications and parameters of several usualy board CPU system.[49]

Parameters	Arduino uno	Mega 2560	Microbit	Arduino Due	ESP8226	ESP32wroom	M5stack Basic
CPU	Atmega 328P	Atmega 2560	Nordic nRFS1822	AT91SAM3X8E32-bit	Xtensa Single core 32-bit	Xtensa Dual core 32-bit	ESP32 dual core, 600 DMIPS
Clock	16MHz	16MHz	16MHz/64MHz	84MHz	80MHz	160 à 240MHz	240MHz
Input voltage	5v	5v	3v	5v	3v	3.3v	3.3v
Supply voltage	7-12V-200Ma	3-5V-200mA	7-12V-200mA	5V	5V	5V@500mA	
GPIO	16	54	20	54	17	36	36
Input/outputNum/anal	14/6	54/6	20/6	53/2	18/1	18/2	16 No use
Input/output UART	1	4	0	4	0	3	3
Input/output I2C	1	1	1	2	0	2	2
Input/output SPI	1	1	1	1	0	3	3
(flash) Memory	32Ko	256Ko	256/512KB	512KB	4MB	>4MB	4MB
(Sram)Memory	2Ko	8Ko	16/128KB	92KB	64KB	520KB	520KB
Usb interface	USB-B	USB-B	Micro - USB	USB-B	USB-C	USB-C	USB-C
Wifi					Wifi :802.11b/g/n	Wifi :802.11b/g/n	Wifi :802.11b/g/n
Bluetooth			Bluetooth4.0 LE			Bluetooth4.0 LE	Bluetooth4.0 LE
Size	68x53mm	101x53mm	42x53mm		48x25mm	48x25mm	54x54x18mm
Sensor	NONE	NONE	2buttons,magneto Accelerometer, T,LUM		Hall effet/ accelerometer	Hall effet	3buttons, magneto Accelerometer
Display			5x5 leds				Display 320x240 HP1W,SD card sl
Price	3-20€	4-40€	15-20€	32-52€	3-10€	3-10€	25-35€
IDE	Arduino/Blocs	Arduino/Blocs	Python/Blocs	ArduinoPython/Blocs	Python/Blocs	Python/ArduinoBlocs	Python/ArduinoBlocs

the human body, the time separating the emission from the reception of the ultrasound pulse makes it possible to know the depth of the target. Ultrasonic sensors use sound vibrations whose frequencies are not perceptible to the human ear. Frequencies commonly used in this type of technology range from 20 kHz to 200 MHz.The ultrasounds emitted propagate in the air and are partially reflected when they hit a solid body, depending on its acoustic impedance. In the human body, the waves will propagate at a speed close to 1500m/s-1 depending on the nature of the organs crossed.[50] We use it in sensor JSN-S04T.

Processing of signals resulting from sensors (Figure 2C)

FECGSYNC-BD database

This database is an international reference used by researchers to test cardiac treatment medical devices. It contains recordings of numerous maternal and fetal electrocardiogram signals obtained using electrodes. The patients who participated in this study gave their consent and authorized free access to their data. Additional information can be found on website. We will use this database for the clinical validation of our device.

Blind separation of sources

Blind source separation (BSS) relies on estimating multiple source signals from their observed mixtures, despite the fact that little information about the mixtures is known.[15] Our mixed signal has as main components: the fetal heart signal (FECG), the maternal heart signal (MECG) and other noises.

The basic principle of the improved SOBI signal de-nosing method based on a time correlation of the source signal and the joint approximation diagonalization of the covariance matrix. When it applied to signal de-noising, the noise information is separated and zeroed by the other two sets of data, and the mixed matrix is used to inversely reconstruct the signal to obtain the de-noised signal. The figure 4 shows the entire workflow of the improved SOBI signal de-noising method for the obtained time-series displacement of bridges using FECGSYND. The workflow includes the following four key technologies: (1) the observation signal, X (t), whitened to obtain a unit matrix covariance matrix, Z (t). The second-order correlation among the signal components removed, and the sampling covariance matrix of the whitened data, Z (t), is calculated. (2) The orthogonal matrix obtained using joint approximate diagonalization of the covariance matrix with different time delays. (3) The estimated value of the source signal, Y (t), and the mixing matrix, A, are calculated using the orthogonal matrix. (4) The estimated value of the source signal, Y(t), is converted in the frequency domain using the fast Y t , is converted in the frequency domain using the fast Fourier transform (FFT), and the noise signal component is identified using the frequency characteristics. A new independent separated signal component matrix, Fourier transform (FFT), and the noise signal component is identifie dusing the Frequency characteristics. A new independent separated signal component matrix, $Y_Z(t)$, is generated using a zeroing process for noise signal components, which is inversely reconstructed using a mixing matrix, A, to recover the original amplitude of the de-noised signal, $Y_N(t)$. Y t, is generated using a zeroing process for noise signal components, which is inversely reconstructed using a mixing matrix, A, to recover the original amplitude of the de-noised signal, Y_N (t).

The principle of BSS can be represented in *Figure.3.A*, it involves finding in the ideal case the matrix W of size n x m which provides the output vector:

The simplest filtering of a time series involves the transformation of a discrete one dimensional (N = 1) time series x[m], consisting of M sample points such that x[m] =(x1, x2, x3... xM)T , into a new representation, y = (y1, y2, y3... yM)T . If x[m] (T = 1,2, ..., M) is a column vector6 that represents a channel of ECG, then we can generalize this representation so that N channels of ECG X, and their transformed representation Y are given by:

$$Y^T = WX^T = WHS^T \quad ...(7)$$

The estimated sources are obtained from the vector and their associated projections for the different sensors are determined from the estimated mixing table 4:

$$H = W^{-1} \quad ...(8)$$

$$X=\begin{bmatrix} a & b \\ c & d \end{bmatrix}\begin{bmatrix} S1 \\ S2 \end{bmatrix}=HW \quad ...(9)$$

It has been proven in that the efficiency of the BSS algorithm is measured by observing the value of the separability index (SI), [16, 17] through the following equation:

$$SI = \frac{1}{n(n-1)}\sum_{i=1}^{n}\left\{\left(\sum_{k=1}^{n}\frac{|g_{ik}|}{max_j|g_{ij}|}-1\right)+\left(\sum_{k=1}^{n}\frac{|g_{ki}|}{max_j|g_{ji}|}-1\right)\right\} \quad ...(10)$$

The elements (i, j) of the global matrix of the system.[19]

$$G = WH \quad ...(11)$$

and $max_j\ (g_{ij})$ the maximum value of the elements of the ith row vector of G. In the same way has the maximum value of the jth theme of the line vector G.

Software connectivity of our device. Set up and Configure ESP32 Hardware[50]

Once you have installed the MATLAB support package for Arduino Hardware, as described in the "Installing the Support Package" section, you can configure communication between your computer and the ESP32 board. Type "arduinosetup" in the command window and choose the connection type between USB, Wi-Fi, or Bluetooth. Select the Arduino-compatible ESP32 version from the Simulink hardware options menu and, using the pin configuration tool, connect the other components.

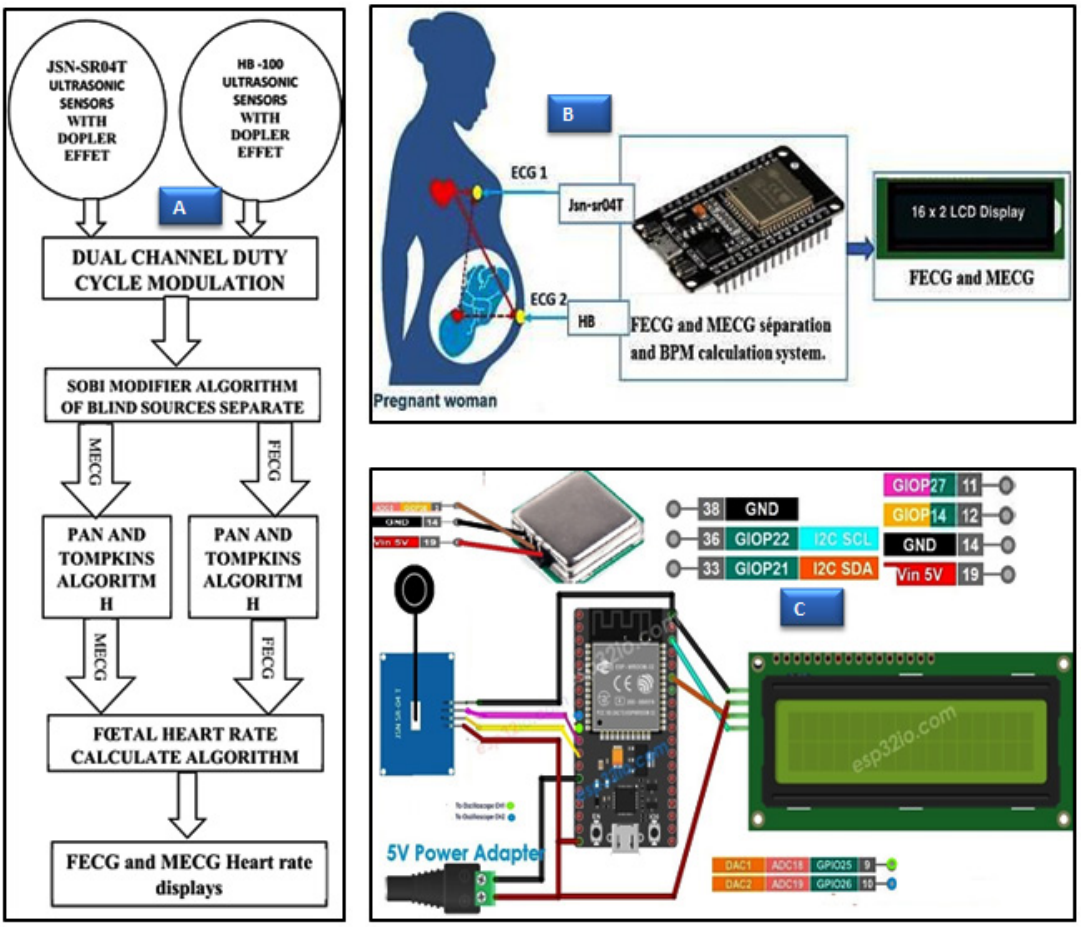

Fig. 2. A (Technical Synoptic diagram of our device). B (Material Synoptic diagram of our device). C (All practical connections of the complete print circuit board).

Detection of QRS Complex and calculation of BPM

Here, we will use algorithms based on derivative and digital filtering. The most used is that of Pan and Tompkins.[32] Known as *(Figure.3.C)*. Indeed, in 1985 they proposed a detection method presented in Figure 3c, the steps of which are: Band-pass filtering, derivative filtering, non-linear transformation and integration. However, this method has the disadvantage of detecting P or T waves in the case where they have large slopes and amplitudes. It was then that in 1990 modified this method by retaining just the derivative and low pass filtering and subsequently defining an

Table 2. Describe all type of physiological dataset in FECGSYNDB

Baseline	Abdominal mixture (no noise or events)
0	Baseline (no events) + noise
1	Foetal movement + noise
2	MHR /FHR acceleration / decelerations + noise
3	Uterine contraction + noise
4	Ectopic beats (for both foetus and mother) + noise
5	Additional NI-FECG (twin pregnancy) + noise

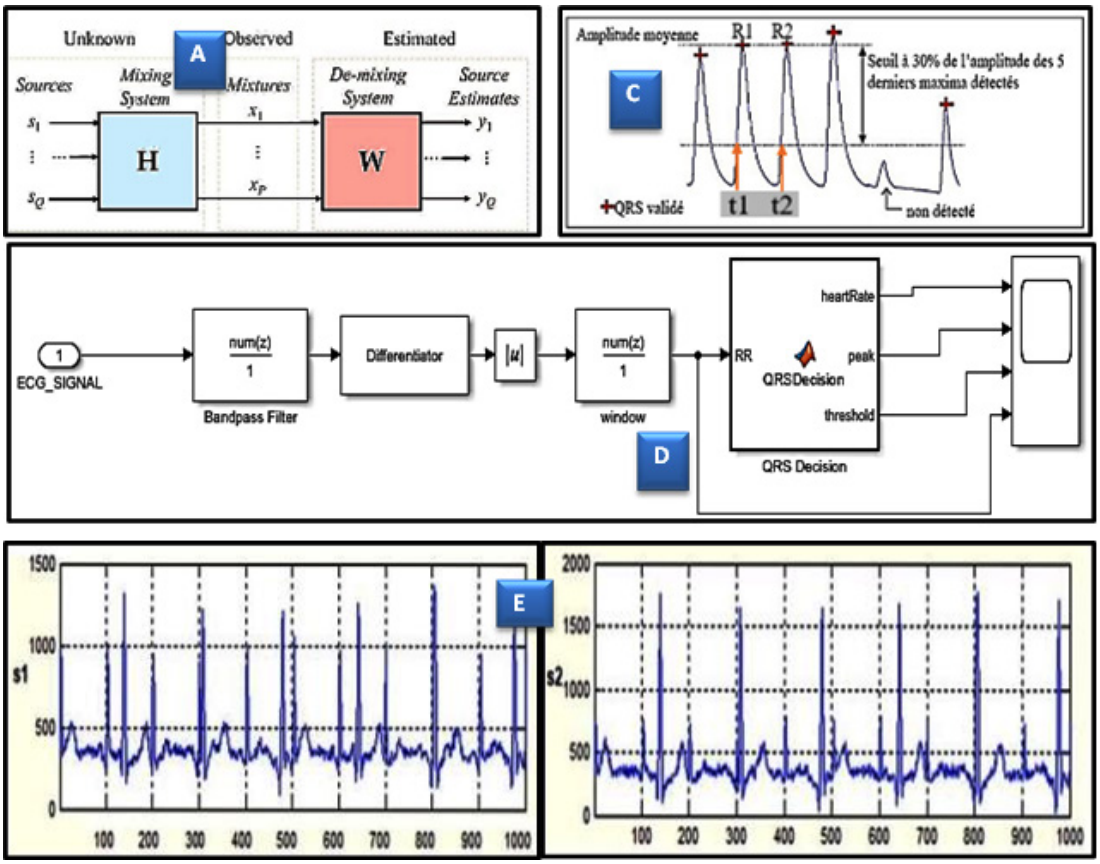

Fig. 3. A (The figure shows the principle of the separation of sources).[28] B (Thresholding and detection of R peaks). C (The QRS complex detection chain carried out in Matlab/Simulink). D (The ûgure shows an ECG of a pregnant woman (s1 from Thorax; s2 from Abdomen)).

amplitude threshold and a temporal threshold allowing the peaks to be detected. But this does not completely guarantee the non-detection of possible P and T waves. To remedy these disadvantages, adaptive threshold systems is developed allowing the threshold to be adapted to each amplitude of the R wave acquired.

Most of the spectrum of a QRS complex is located in the frequency range 5 to 30 Hz. It is therefore highly useful to filter the ECG signal collected in order to eliminate all added parasitic noise and retain only the frequencies of the complex.[43] A high pass filter will remove baseline ripples and some artifacts. A band pass filter will also eliminate muscle noise and the 50/60 Hz signal from the power supply network. Regarding the design of digital filters, most algorithms propose band-pass filters.[36] Generally speaking, the filter response can be put in the form.

$$\begin{cases} y(n) = \sum_{i=n-N1}^{n-1} a(n-i)y(i) + \sum_{j=n-N2}^{n} b(n-j)x(j) \\ y(k) = a0x(k) + a1x(k-1) + a2x(k-2) - b1y(k-1) - b2x(k-2) \end{cases} \quad ...(12)$$

The coefficients (a) and (b) and the orders N1 and N2 must be determined according to the nature of the filter, the cutoff frequencies, and the passbands.[42] The function of the filter is to reject the noise and retain the useful signal. Finally, the reconstruction of the signal is done using a second-order low-pass digital RII filter obtained by the discretization by Tustin of the analog filter whose expression is given by (13):

$$\begin{cases} F_c = \frac{K_f w_n^2}{S^2 + 2\gamma W_n S + W_n^2} \\ K_f = \frac{1}{2\beta E} \end{cases} \quad ...(13)$$

With K, f, the static gain, the table of

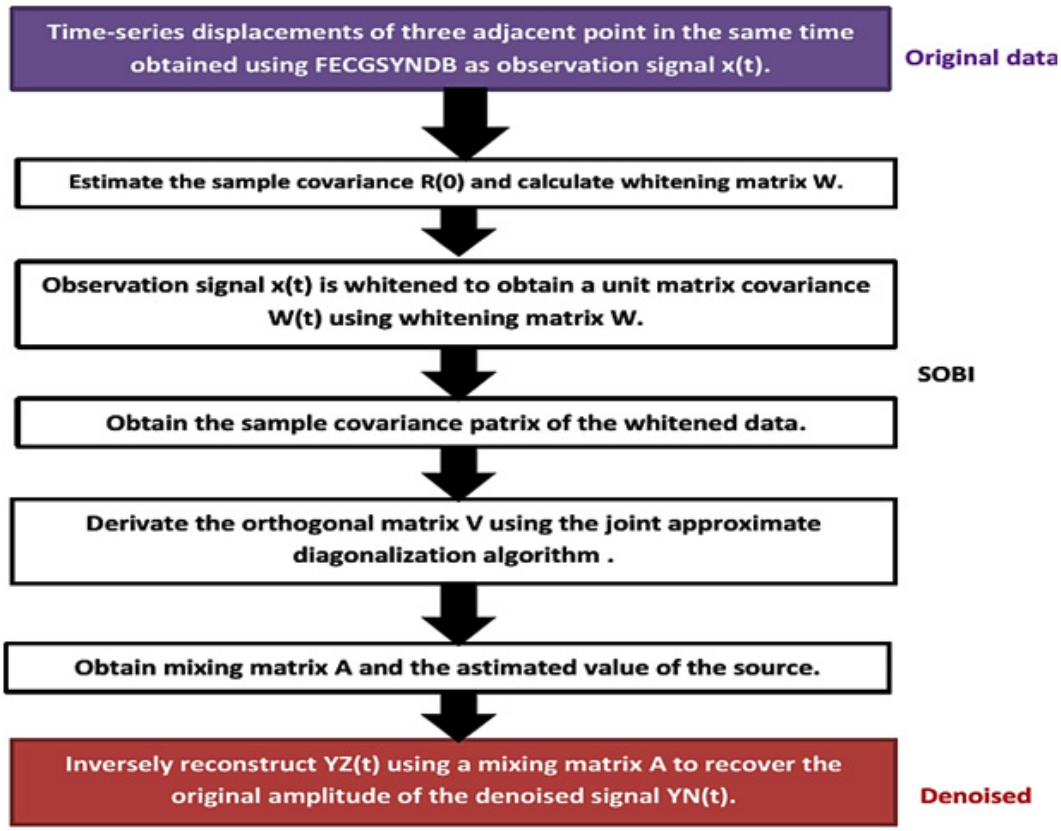

Fig. 4. The basic principle of the improved SOBI signal de-nosing method and filtered

simulation values given in the result section.

First and second derivatives of the filtered signal

The first derivative makes it possible to obtain the variations of the signal. A steep positive slope followed by a steep negative slope characterizes the R wave. Instead of the high-pass filter, we will use a band-pass filter whose gain will be close to the high-pass filter in the range of frequencies below 30/40Hz and quickly attenuating frequencies beyond. The transfer function of such a digital bandpass filter allowing the signal to be derived is for example:

$$H(z) = \frac{1}{8T}\ (-z^{-2} - 2z^{-1} + 2z^{1} + z^{2}) \qquad ...(14)$$

The frequency response is:

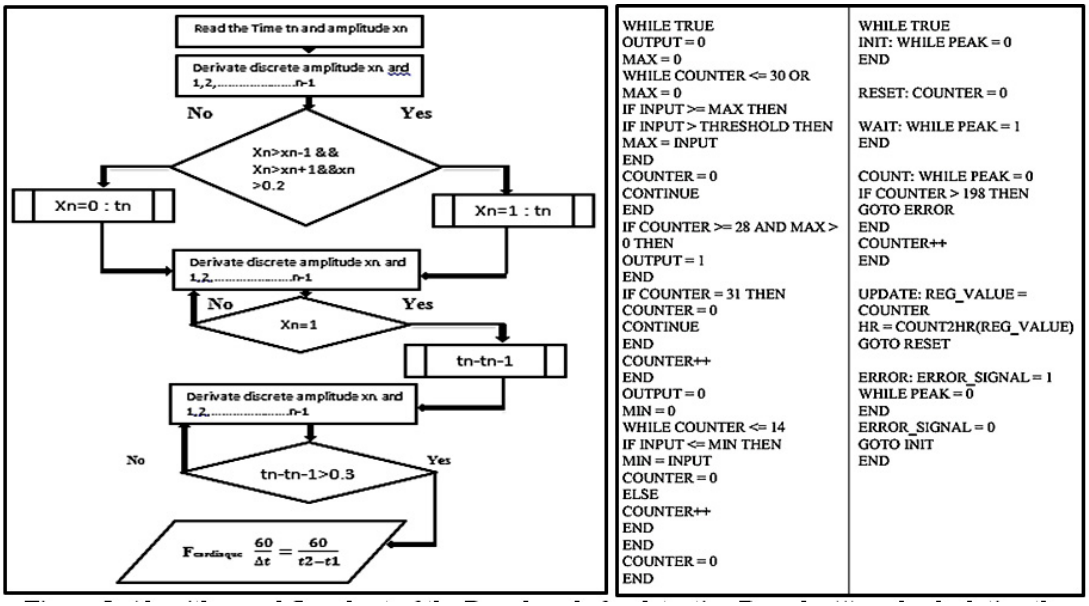

Fig. 5. Algorithm and flowchart of the Pseudocode for detecting R peaks (1) and calculating the heart rate (2) proposed in our work.

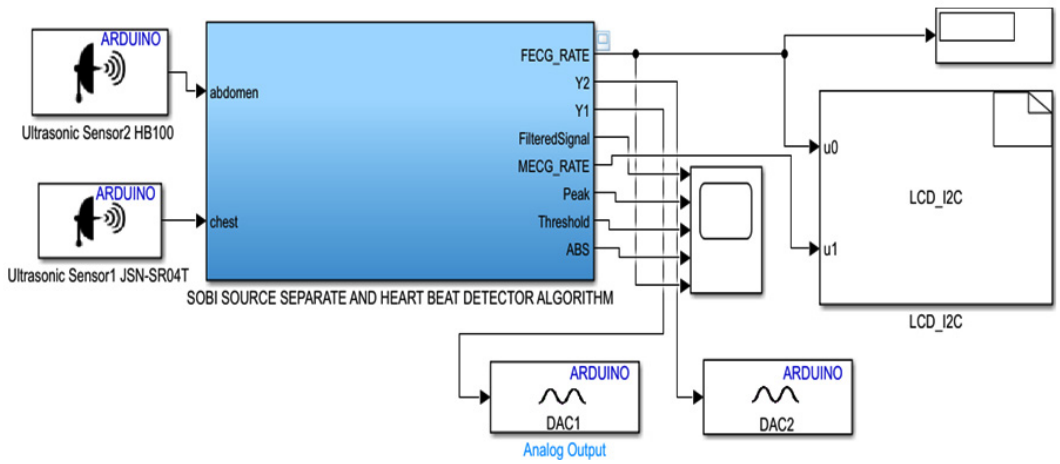

Fig. 6. (overall diagram of the software configuration of our device on Matlab/Simulink and Hardware Real Time configuration of all components of our device).

$$|H(2\pi ft)| = \frac{\sin(4\pi ft)+2\sin(2\pi ft)}{4T} \quad ...(15)$$

In a simpler and widely used way, the first numerical derivative is defined by the difference in the values of the upper and lower indices D1 (n) = x (n+ 1) - x (n- 1),

The recurrence equation of the derivative filter is given by:

$$y(n) = x(n) + 2x(n-1) - 2x(n-3) - x(n-4) \quad ...(16)$$

Energy collector and averager

The energy collector is a nonlinear operator making it possible to increase the contrast of the signal and obtain a positive signal; the simplest collector is the absolute value.[40]

Envelope of a signal

The envelope of a signal is defined as the modulus of the analytical signal:

$$x^*(t) = x(t) + j\,x(t) \quad ...(17)$$

The real part is the signal whose envelope we wish to determine. The imaginary part is the Hilbert transform of the signal x(t), defined by the Hilbert convolution product of the signal x(t):

$$x(t) = \frac{1}{\pi t} * x(t) = \frac{1}{\pi}\int_{-\infty}^{+\infty} \frac{x(\tau)}{t-\tau}\, d\tau. \quad ...(18)$$

The envelope of the signal x(t) is then the modulus:

$$r(t) = |x(t)| = \sqrt{x(t)^2 + x(t)^2} \quad ...(19)$$

Decision rules on adaptive thresholding or not

When the ECG signal has been filtered, its derivatives are extracted, the module of which is taken, and a signal called resultant is obtained, the amplitude of which is normally high during a QRS, and low elsewhere. It is then that one must decide on candidate QRS complexes. The decision rules are based on comparisons with thresholds of the resultant, the amplitude of the ECG signal and other intermediate signals. The QRS complex detection chain is then summarized in the *(Figure.3.C)* .The QRS complex detection chain carried out in Matlab/Simulink.

Indeed, physiologically, we cannot have two consecutive complexes separated by less than 200 ms except in cases of flutter and fibrillation (heart rate > 300 bpm). If a QRS appears in a period of 200 ms to 360 ms (heart rate 170 bpm to 300 bpm), it may be the T wave.[39]

In order to avoid missed detection, it is possible when a QRS has not been found within 166% of the average RR interval.[41] To detect the maximum peak in this time interval following the last QRS detected, and to consider this peak as a plausible QRS. A disadvantage of this technique is the irregularity of the heart rhythm.[38, 40] If we know the times t_1 and t_2 of the R_1 and R_2 waves (*Figure.3.B)*, then we can calculate the heart rate by:

$$F_{cardiaque} \quad \frac{60}{\Delta t} = \frac{60}{t2-t1} \quad ...(20)$$

The performance of such an algorithm is evaluated by the parameters: TP (True Positive) representing the number of R waves correctly detected. FP (False Positive) the number of noise detected as peak and FN (False Negative) the number of R waves not detected. Se (sensitivity) the ratio of True Positives and DER (Detection Error Rate) the error of the proposed method.[45] The results are reported in Table 6.

RESULTS

Hardware configuration results

The (Figure.2.C) schows all practical connections of the complete print circuit board ESP 32, and the (Figure.6) shows all connections of the complete Matlab/Simulink setup of our device.

FHR criteria for validating the decision algorithm

Gestational age for a FHR: The physical activity of the fetus is felt significantly from this moment. Generally, the third month of pregnancy.[49] The second trimester marks the beginning of heart rate differences, which are low during the stages of the nycthemeral cycle.

Night cycle: This is the variation in FHR during the night.[45] It is more important during rapid sleep than during rest phases; these phases are described as follows:

• Calm sleep: Stable rhythm, oscillations may be significant, accelerations rare.

• Restless sleep: Slower rhythm, sharper oscillations, and accelerations those are more frequent.

• Calm awakening: Stable rhythm, calmer oscillations, no accelerations.

• Awakening agitated unstable rhythm, numerous accelerations.

Fetal cardiac arrhythmias are indicative of many pathologies,[50] FHR must be studied judiciously by a health specialist in order to promote its rapid intervention and save the life of the fetus. Numerous definitions have been given for each of the FHR interpretation criteria and various classifications have been established in order to interpret the plots. [48]

In the United States, the American College of Obstetricians and Gynecologists (ACOG) adopted in 2010 the definitions of the FHR interpretation criteria defined by the National Institute of Child Health & Human Development (NICHD, 2010). It is this criterion, which will attract our attention and will serve as a reference for the design of the decision algorithm of our device.

• Normal : if the FHR] 110-160 [BPM

• Tachycardy : if the FHR > 160 BPM

• Bradycardy : if the FHR < 110 BPM

Not all babies have the same rhythm, but if the recording shows abnormalities (slowing down of heartbeat during contractions, slight variations, etc.).[47] This may be a sign of fetal distress. The medical team will then intervene quickly, and most often perform a cesarean section.

Hardware and software configuration of our

Table 3. Pourcentages of CPU utilization during a simulation of ours device

Time(s)	CPU Utilisation (%)
0,5	13
1	11
1,5	14
2	10
2,5	7
3	5
3,5	18
4	22
4,5	26
5	24
5,5	21
6	27
6,5	31
7	32
7,5	30
8	33
8,5	31
9	32
9,5	30
10	29

Table 4. Performance indices of our modified SOBI source separation algorithm. We can use it for reproducibility of our device

Algorithm	Execution Mode	PI	SI
SOBI	Simulation on Matlab	0,0012	78,56
	Real-time implementation on ESP 32.	0,0019	80,12

Table 5. Presents the coefficients of the separation and mixing matrices of our signals for our source separation algorithm Mixing matrix (H); Separating Matrix (W) and Error of our BSS. We can use it for reproducibility of our device

Original signals	Mixing Matrix (H)	Separating Matrix (W)	Error
S_1 = 1000 Hz	1 0.7	1 -0.7011	W_{12} = 0.0011
	0.8 1	-0.8101 1	W_{21} = 0.0101
S_2 = 1000 Hz	1 0.2	1 -0.1045	W_{12} = 0.0955
	0.4 1	-0.3121 1	W_{21} = 0.0879

device

We used the following software and harware éléments:

• Windows 10 operating system and Matlab/ Simulink 2023b software.

• Computer: Hp Intel®core™ i5-4210U CPU@1.70-2.40GHz ; 12Go RAM.

• Dual Chanal analog oscilloscope OS-5030, 30MHz.

• ESP 32 board.

Table 6. Presents all the sizing parameters of our filters, duty cycle modulator for the Pan and Thomkins algorithm used while. We can use it for reproducibility of our device

2^{nd} order pass band filter : Fc = $35Hz$ and Fs = 25MHz						Derivator filter				
a_0	a_1	a_2	b_1	b_2	kf	a_0	a_1	a_2	a_3	a_4
2.352^{e-10}	9.1105^{e-10}	2.352^{e-10}	-1.9217	0.9217	1.5624	1	2	0	-2	-1

System Data	Analog Duty cycle modulator				
	α_1	α_2	τ =RC	E	Fm(0)
parameters	0.19902912; R1=8.2K; R1=33K	0.800970873	R=1K; C=22nF	5V	58Khz

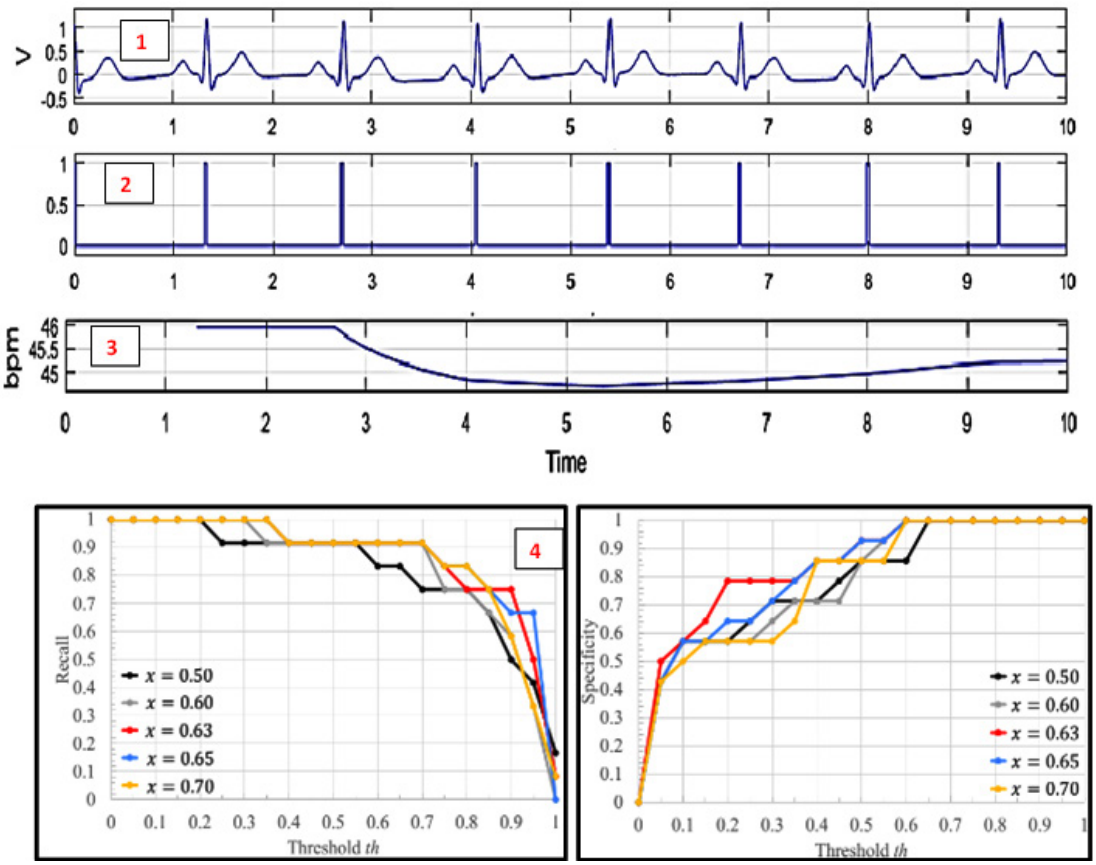

Fig. .7. (1) Filtered, differentiated and absolute value ECG signal. (2) Essential points and Signal_R and Reference. (3) Heart rate calculation. (4) Peformance of ourn DCM with differents values of accuracy and sensitivity

Table 7. Result of real time simulation of 30 patients volunters in several clinical center in Cameroon

(PN)	(AOM -year)	(GW+D)	(GOBM)	(MHBFOD-BPM)	(MHBFRD -BPM) 7MHz	MBHE (%)	(FHBFOD-BPM) 4MHz	(FHBFRD -BPM) 7MHz	FHBE (%)
1	18	22+3	M	76	72	5.26	152	155	1.97
2	22	23+1	M	76	72	5.26	157	156	0.63
3	24	24+6	M	79	78	1.26	163	164	0.61
4	32	25+4	M	85	87	2.35	153	150	1.96
5	36	25+3	M	82	84	2.43	149	156	4.69
6	17	27+1	M	84	85	1.19	145	149	2.75
7	26	28+6	M	71	78	9.8	131	138	5.54
8	24	29+4	M	78	80	2.56	164	167	1.82
9	41	30+2	M	89	96	7.86	152	158	3.94
10	36	31+2	M	91	89	2.19	144	159	10.41
11	34	32+1	M	87	86	1.14	134	135	0.74
12	23	33+5	M	84	90	7.14	158	157	0.63
13	22	34+5	M	83	84	1.20	136	136	0
14	35	35+4	M	78	79	1.28	140	143	6.47
15	20	36+0	M	79	76	3.79	139	148	6.47
16	35	22+6	F	75	76	1.33	154	158	2.59
17	19	23+5	F	88	87	1.13	162	169	4.32
18	23	24+6	F	87	89	2.29	160	177	10.62
19	34	25+1	F	79	90	13.92	148	145	2.02
20	32	25+0	F	76	78	2.63	146	148	1.36
21	24	27+1	F	93	93	0	158	156	1.26
22	18	28+4	F	78	75	3.84	169	169	0
23	19	29+2	F	90	97	7.77	171	178	4.09
24	27	30+5	F	86	86	0	167	166	0.59
25	28	31+4	F	83	84	1.20	165	165	0
26	20	32+2	F	77	80	3.89	178	177	0.56
27	40	33+6	F	69	74	7.24	143	144	0.69
28	23	34+6	F	70	70	0	132	132	0
29	27	35+3	F	83	83	0	145	144	0.68
30	19	36+3	F	82	82	0	155	157	1.29

LEGEND :
Patient Number (PN).
Age of Mother (AOM-year).
Gestational Week+days (GW+D).
Gender of Baby Male or Female (GOBM).
Mother's Heart Beat for Our Device (MHBFOD-BPM).
Mother's Heart Beat for Reference device 7MHz (MHBFRD-BPM).
Maternal Heart Beat Error (MBHE %).
Fetal Heart Beat for Our Device (FHBFOD-BPM) 4MHz.
Fetal Heart Beat for Device Reference (FHBFRD-BPM) 7MHz.
Fetal Heart Beat Error (FHBE %).

• SPSS 31 for statistical analysis for windows 10 operating system.
• Microsoft Office 2013.

Results of simulation

The results of the simulations seen from the Matlab/Simulink scopes are recorded in Figure 7.

Implementation results

After simulating our device in the Matlab/Simulink software, we compiled the program and loaded it into our ESP32. For the validation of our device, we chose two patients groups:

• Group of Patient 1: female fetus; intrauterine single-fetal pregnancy normally progressing at [22-39] weeks of gestation.
• Group of Patient 2: male fetus; intrauterine single-fetal pregnancy normally progressing [22-39] weeks of gestation.

The following figures and tables show the results of the display of our device on LCD_I2C in comparison with those of the obstetric ultrasound records of each patient carried out in various hospital facilities.

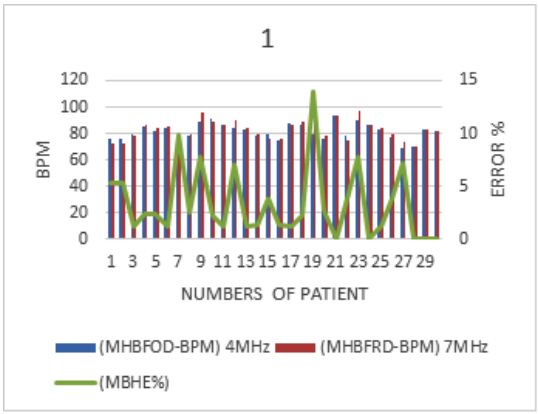

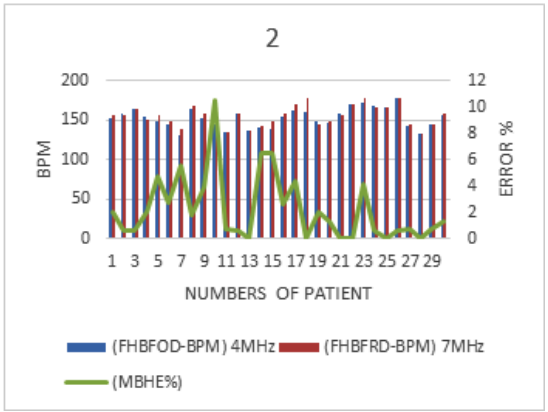

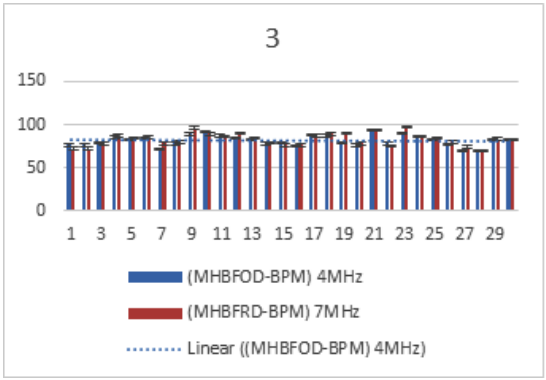

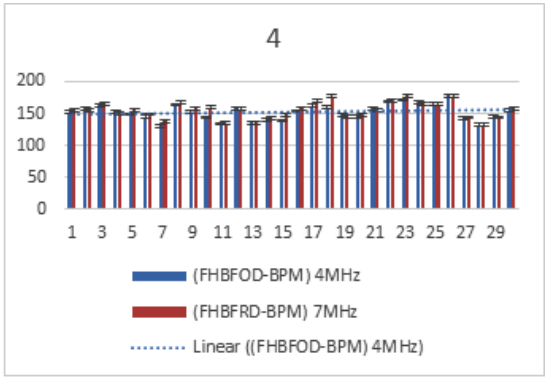

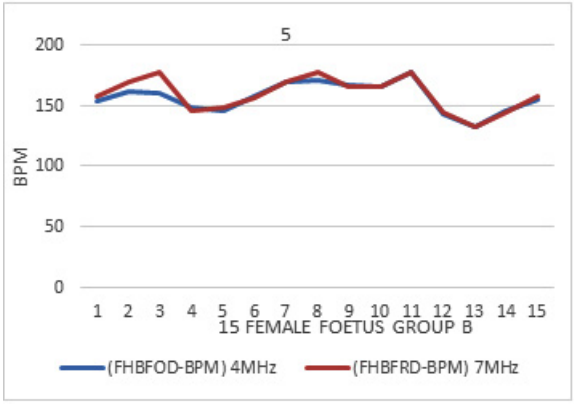

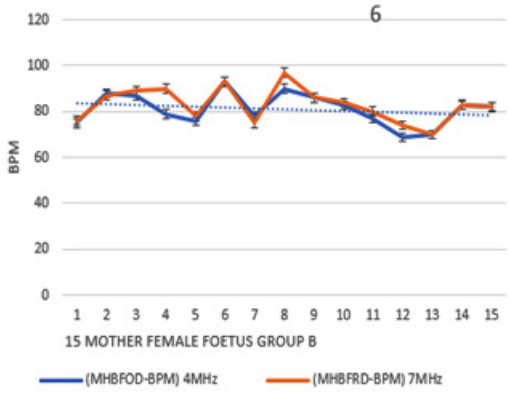

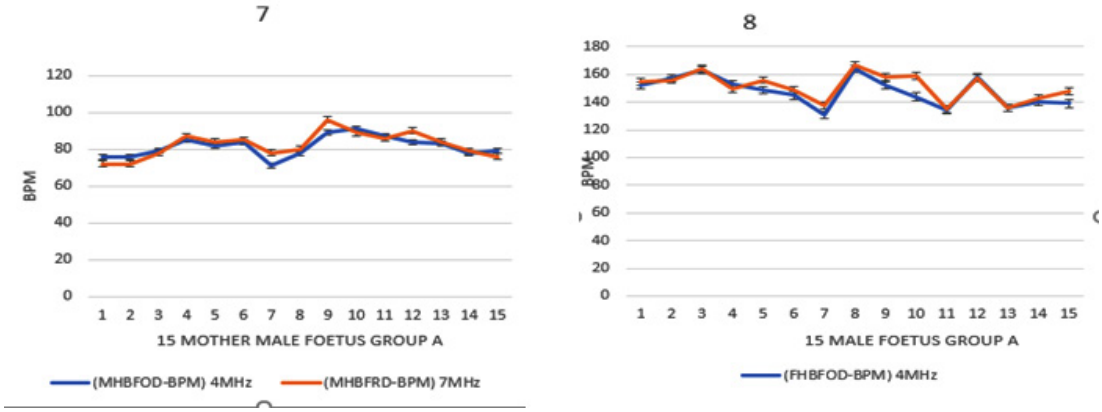

Fig. 8. (1) (3) comparison between the eadings of our device and that of the reference heart rate of thirty pregnant women. (2) (4) comparison between the readings from our device and the reference heart rate of thirty fetuses from previous pregnant women. (5)(6) Comparison between the readings. from our device and the reference heart rate of group A. (7) (8) Comparison between the readings of our device and that of reference heart rate of group B.

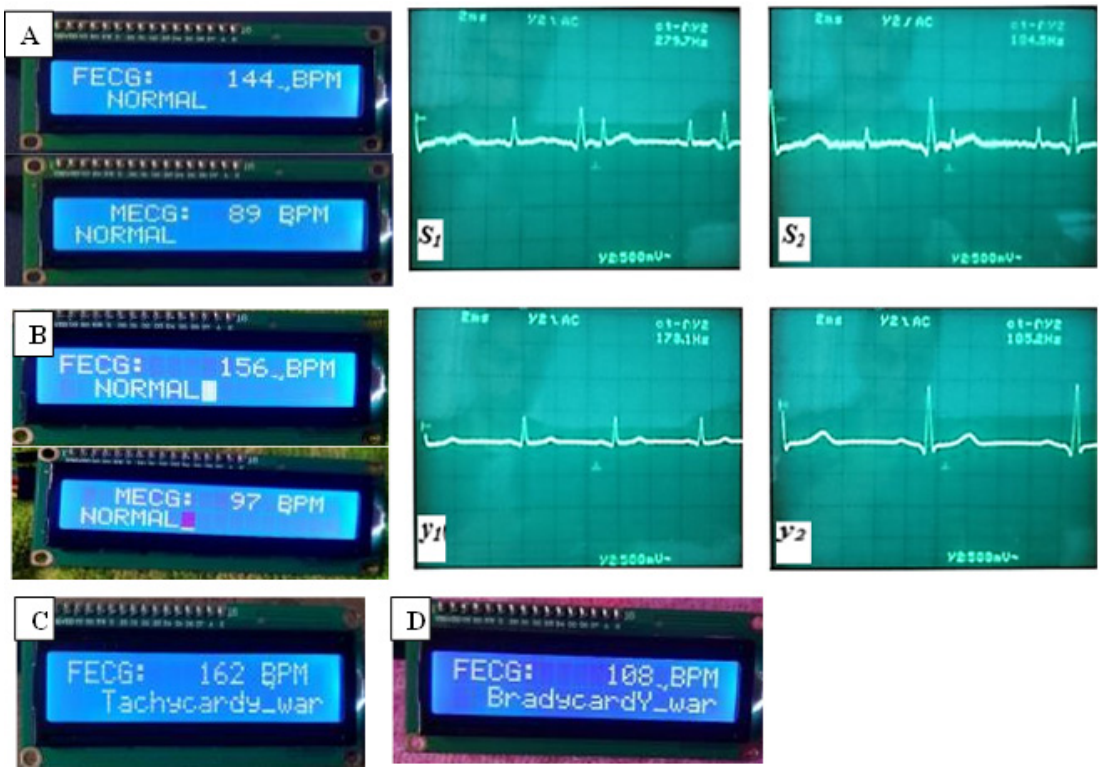

Fig. 9. Result of the display of our device and the obstetric ultrasound chart (A and B = Normal working) of several patient 2. Result of the functioning of our decision algorithm, tachycardia (C) and bradycardia (D). Real-time result of blind separation extraction result: Source signal S_1; Source signal S_2; estimated signal y_1 (FECG); estimated signal y_2 (MECG)

$$\begin{cases} SE = \frac{TP}{TP+FN} \\ \text{DER} = \frac{FP+FN}{TP} \end{cases} \quad ...(21)$$

DISCUSSION

Blind sources Separate discussion

The results of the real-time implementation on our ESP32 Woom (Figure.7. (1….6)) show ECG curves similar to those obtained through simulation on Simulink, which confirms the accuracy of the SOBI method we used. The parameters of matrix (A) and the optimal error margins for our model are recorded in tables 5. It observable through the assumptions of our internal similarity function block among the 9 expected signals, since these were morphologically closer to the expected references (Table 8). The performance and separation indices were evaluated using the signal-to-interference ratio (SI=80.12; PI=0.0019) (Table 4) and their impacts on the fetal signals from the FECGSYND database (Table 9). The real-time analysis of our decision algorithm is presented in (Figure.8.A, B, C, and D). The comparative results betwenn our device and a reference portable cardiothocography device in shows in figure 8. We can see all confiance intervals and the parameters while the second is a dataset of 30 volunteer patients from district hospitals in Cameroon (Table 7). The volunteers were informed about the nature of the research and the use of the acquired data, and gave their consent regarding their purpose. These real tracks were acquired using the portable prototype described in our synopsis. We processed the synthetic and real input samples in the adapted integrated RAM memory of our ESP 32 WROOM (Table 3).

After separating each track into nine

Table 8. Performnace comparison of PCA-whitening; ICA and SOBI

Parameter	PCA-Whitening		ICA		SOBI	
	MECG	FECG	MECG	FECG	MECG	FECG
Kurtosis	21.3044	4.0675	25.7665	9.7686	30.6390	11.3409
Skewness	3.6789	-0.077	-4.1234	-0.6087	-6.7681	-0.4536
Entropy	2.9533	5.8143	4.9488	4.7543	5.6540	6.0121
SNR (db)	-8.5324	0 .1232	-11.4563	-8.5646	-12 .0011	-10.3409

Table 9. Summary of the results of arrhythmic and normal ECGs from FECGSYND

Class Name R peak	Recall	Precision	F-score
Normal	0.991	0.993	0.998
Suspect	0.973	0.961	0.972
Pathologic	0.994	0.994	0.994
Weighted Average	0.990	0.991	0.992
Accuracy	99.2004%		

Table 10. Summary of results for Matlab ECG sources for the fetus

Signal	number of R waves detected	TP	FP	FN	SE%	DER%	Fetal heart rate (Bpm)
160 (Bpm)	27	36	0	1	96.29	3.84	156
220(Bpm)	36	32	0	4	88.88	12.5	217
110 (Bpm)	17	16	0	1	96.29	1.13	108

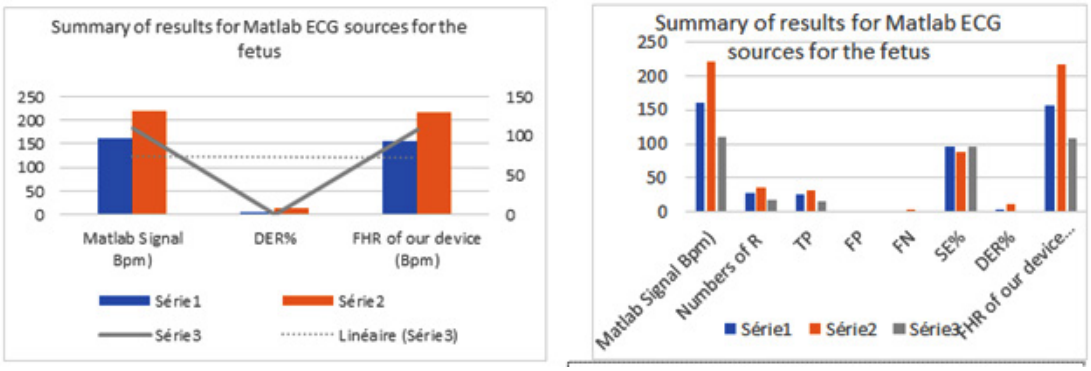

Fig. 10. Comparative result between Matlab ECG sources and FHR of ours device.

channels, there is always at least one channel containing the fetal signal. This channel is determined by the separation matrix (Table 5), which randomly tests the values to achieve the desired accuracy. The comparative parameters for tirth methods are shown in (Table 8) for the best simulation using M=9CHs.Our SOBI shows better results in terms of kurtosis revealing the super-Gaussian nature of both the MECG and FECG. Especially, for the FECG, the improvement for the SOBI is significant with a value of 11.3409. The performance is better in the ICA for the FECG in terms of skewness and entropy as well. However, the same parameters give better results for the MECG with the PCA-Whitening. The SNR calculated for the FECG with the SOBI shows a significant improvement of -10.3409dB while the same for the PCA-Whitening is only 0 .1232dB and -8.5646 for ICA. For the MECG, the SNR values are almost comparable to 8.5324Db and 10.3209 dB for the PCA-Whitening and SOBI respectively with the SOBI an insignificant improvement.

Our chip's CPU utilization is less than 15% (Table 4) for logic elements, less than 3% for total memory (1,668,714 blocks), and approximately 44% for onboard multipliers (122). The operating frequency is 95 MHz. Estimated power consumption is less than 468 W, making it compatible with the constraints imposed by a portable system. The processing time depends on the number of SOBI iterations, the number of turning points and the iteration required for the clustering phase. We therefore note that at the working frequency of 95 MHz, this corresponds to a processing time of 1.8 ms to 27 ms. the real-time constraint is respected, because the tracks used are about 4s. By changing the parametric values of the matrices of our SOBI algorithm, we have 120 ms to separate the sources; our implementation is therefore faster than those of the literature reviews in our comparison table. The energy consumption decreases to about 550 mW, with a maximum processing time of about 54 ms, values higher than the solution proposed in (table 11) while remaining compliant with real time.

Regarding the implementation carried out in (table 11), the development times are faster, but the adopted technique is not a BSS approach, which reduces the separation quality. In addition, the power consumption is 1 W, the authors of having announced a current absorption of 200 mA and a component power supply of 5 V.

Hyper parameters and cross validation

A relative balance is observed between the measurements of our device and those of our reference device. It therefore emerges that: 97% of R peak detector even signals despite difficult conditions (skin; intestines, blood circulation, amniotic fluid of the mother). The Accuracy = 99.01 (%). Sensitivity = 97.45 (%). Specivity =97.09(%). Precision = 98.11 (%). F1 Score = 96.89 (%), beter than several authors in literature review Table 9. The best parameters of each block given on table (4- 5- 6). On the figure 7-4, we can see better values on x parametters and thers differents inpacts in recall and specificity.

Operation of our classifier

We confirm the real-time operation of our classifier, which provides information on an LCD display of the fetal health status (Figure.9.

Table 11. Comparison of some parameters resulting from our work with several existing work

Method	Database and test mode acquisition	Recordings	Year	FHJR presision%	SE%	Estimated cost (USD)	PI	Sampling frequency	Boards
Proposed work	FECGSYNDB MATLAB Real time	25 4 30	2025	97	97.29	52.57	0,0011	1000 Hz	ESP32 wroom Ultrasonic
SYM-WHITE (Mekhfioui et Al) [18]	FECGSYNDB Real time		2024	97	95.23	80 ,5	0.0012	1000 Hz	ESP 32 Arduino Due AD8232
CA-KICA (L. Qiao) [23]	ADFECG NIFECGCA	5 69	2023		98.4 99 .3	107	0.0018	512 Hz	
DEEP LEARNING (Choodamani Bhattarai et al)[42]	MATLAB MIT-BIT Real time	4 6 2	2022	97	98	80	-	1500 Hz	ESP32 wroom AD8232
DPSS (Negar Tavassolian) [47]	NIFECGC ADFECGBD(L)	69 12	2022	83,86 89,22	94,2 98	104		500 Hz	
FAST ICA (K. Sri Vidya) [43]	MATLAB	4	2022	80%		120	0.0021	500 Hz 250 Hz	ESP32 TTGO
NiNFEA (Pani, D. *et al*) [28]	NINFEA MATLAB	394	2021	89	98	-	-	2048Hhz	Philips iE33 Ultrasound Machine
FAST ICA (Soumitra Das) [20]	Real time		2020	100	97	60		250 Hz	ATmega328P Node CMU

Table 12. Component list and cost of each for this system

Component name	Quantity	Unit price (USD)	Total price (USD)
HB100 sensor	1	11.55	11.55
JSN-SR04T sensor	1	7.77	7.77
ESP32 WROOM	1	15.55	15.55
LCD_I2C	1	11.55	11.55
9V battery	1	0.5	0.5
LM7805	1	0.15	0.15
LM 324 module	1	4	4
Essais BOARD	1	3	3
Cable	20	0.25	5
Total cost of the system			66.57

A, B, and C, D). The normal, monitored, and pathological fetal heart rate states are represented with an acceptable confidence interval shown in (Table 4) and (Table 6). These data are uploaded to the card via the USB port and will be processed in the same way if the analog pins of the ESP 32 WROOM card (ADC_1 and ADC_2) receive the data.

Limitations of our study

Our study is limited to the use of two separate sensors for FHR assessment. Despite acceptable metric parameters at an affordable price, the use of synchronized multi-sensor functions will improve the accuracy and depth of our device. The use of artificial intelligence techniques in the overall development of our device. The creation of advanced disease classification databases, and remote monitoring opens the door to future work in this field.

These results are very important because they allow us to compare the frequencies calculated by our algorithm to those of Matlab Table 9. We simulated the 160 bpm, 220bpm and 110bpm sources. Figure.8 presents the graphical processing results for the 160 bpm source case. Profile of graphical processing results from other sources are similar.

The results also demonstrated that our developed IoT system allows patients to have a simple and comprehensive real-time monitoring system for the fetus. They must therefore be compared to some devices using similar algorithms and the following table allows this.

For maternal and fetal channels, aliasing and bandwidth limitations are addressed using analog low-pass filters before sampling at the output of the ultrasound transducers, as shown in Figure 1G, followed by digital signal processing algorithms. Anti-aliasing filters: a second-order analog low-pass filter is placed upstream to eliminate all frequencies above our cutoff frequency (1 kHz), thus preventing aliasing during sampling and the introduction of spurious frequencies. Bandwidth limitation is managed by choosing the appropriate sampling frequency, respecting the Nyquist-Shannon theorem to avoid aliasing and capture all frequencies of interest, and by using digital processing techniques to extract useful information.

Ultrasound energy can potentially produce biological effects on the body. In particular, ultrasound waves can cause slight heating of tissues and One megahertz penetrates to a depth of approximately 3 to 5 centimeters.

When performing the tests, we must pay attention to several parameters: For deep vessels, use a 2 to 3 MHz probe, and for superficial vessels, a 5 to 13 MHz probe is preferable. The Doppler angle should be between 15 and 60 degrees, as 90 degrees provides the maximum signal. Apply the protective anti-burn foam.

Our device is limited to the separation of the FECG and MECG signals embedded, in a mixed signal, to the calculation of the fetal heart rate FHR thanks to the detection of R peaks and to decision.: If the rhythm is normal, to be monitored or pathological (Normal, bradycardia, or tachycardia) taking into account the number of beats per minute BPM. It must be less expensive than those already carried out, which is why a comparative study must have been carried out.

Financial considerations and improvements

An ultrasound costs around 22.22 USD in Cameroon and at least three are needed throughout the pregnancy, therefore a cumulative value of 66 USD which is significantly below the estimated cost of our device, which will be reusable during the next pregnancy and as many times as possible. Several aspects may be taken into account during the future improvement of our project, in particular:

• Communication by wifi, Bluetooth or internet of our results via an Android phone, which may be possible with the same ESP 32 WROOM circuit. This would allow the doctor to be able to obtain his patient's results regardless of the distance and to be able to intervene.

• The future use of several other physiological sensors; temperature (to monitor the temperature of the mother and fetus in real time. Tonometer (to measure uterine contractions and fetal movements)

• The future use of several sensors distributed around the mother's abdomen for a synchronized Doppler emission, because in practice, we have had too much difficulty finding the real position of the fetal heart, thus increasing the anxiety of the patient 2.

CONCLUSION

The objective of the research presented in this manuscript was to create a device for preventing fetal suffering through heart rate analysis, in order to resolve the problem of intrauterine fetal health in the most isolated regions of developing countries: the case of Cameroon. We started from a problem observed in third world countries in general, and in Cameroon in particular: the difficulty of many pregnant women accessing regular medical monitoring. The analysis of this problem revealed on several occasions that these target populations deplored the very high cost of these examinations and the unavailability of monitoring devices in many health centers. To compensate, we considered the use of innovative techniques for the design of a remote fetal monitoring device which represents an improvement over existing devices. We started from maternal and fetal signals acquired using Doppler ultrasound probes, preprocessed using the modified Pan and Thomkins method, then source separation and finally the calculation of the classified fetal heart rate. Matlab/Simulink software was used for configuring our blocks, programming our algorithms, simulation and implementation on multi-core chips such as the ESP32 WROOM board. The latter, thanks to its larger memory, its computing power and the multiplicity of its integrated functions, has enabled the combination of several sensors for maternal and fetal measurement and monitoring.

We used the FECGSYNDB database to test the SOBI algorithms, which validated our method. This database contains electrocardiographic recordings of different pregnant women throughout the nine months of pregnancy.

The real-time tests were carried out on two patients with pregnancies of different stages and male and female fetuses. This made it possible to compare their obstetric ultrasounds, carried out with conventional Doppler devices, to those carried out with our device. The results of this comparison, obtained with clinical equipment, were not perfectly identical. Therefore, for better accuracy, hardware improvements will be required to optimize performance. Finally, the device that we configured and tested in real time on numerous patients in a hospital environment has relatively good characteristics considering its price of 66 USD. With a separability index of 0.0011 and a battery life of 20 hours on a 2,500 mAh battery, it unfortunately only detects 97% of the R peaks of cardiac physiological signals. We plan future improvements in the precision of our work as well as the association of databases with more reliable interpretations of our results thanks to AI.

ACKNOWLEDGEMENT:

We thankfully acknowledge the FECGSYNDB data publicly available and The Research Laboratory of Computer Science Engineering Automation and Bioengeneering, HTTTC, University of Douala, Cameroon.

Funding Source

The author(s) received no financial support for the research, authorship, and/or publication of this article

Conflict of interest

The author(s) do not have any conflict of interest

Data Availability Statement

The author(s) do not have any conflict of interest.

Ethics Statement

This research did not involve human participants, animal subjects, or any material that requires ethical approval.

Informed Consent Statement

This study did not involve human participants, and therefore, informed consent was not required.

Clinical Trial Registration

This trial is registered at [Medical and Bioengineering Center of the Doctoral School of Fundamental and Applied Sciences of the University of Douala, EDOSFA, and Cameroon] with the registration number [BIOENG/201// EDOSFA/2025] dated July 2025.

Permission to reproduce material from other sources

Not Applicable.

Author Contributions

Nguetsop Hermann Beaumont: Visualization, Validation, Software, Methodology. Writing – review & editing, Writing – original draft, Visualization, Software, Project administration, Methodology, Conceptualization; Jean Mbihi: Writing – review & editing, Data curation, Conceptualization; Gamom Ngounou Ewo Roland Christian: Writing – review & editing, Writing – original draft, Visualization, Validation; Moffo Lonla Bertrand: Supervision, Investigation, Data curation, Conceptualization.

REFERENCES

1. World Health Organization. World Health Statistics Monitoring Health for the SDGs, Sustainable Development Goals. *Geneva*: World Health Organization. 2023:01-05.
2. Programme National Multisectoriel de Lutte contre la Mortalité Maternelle Néonatale et Infanto-Juvénile 2014-2020 au Cameroun. *BUCREP*, 2020; 01(9): 7-12.
3. P Hamelmann, R Vuillings, AF Kolen, et al. Doppler ultrasound technology for fetal heart rate monitoring: A review. *IEEE Trans. Ultrasonics, Ferroelectrics, Freq.Control*, 2020; 67(2):226-238.
4. D A Ramli, Y H Shiong, N Hassan. Blind source separation (BSS) of mixed maternal and fetal electrocardiogram (ECG) signal: A comparative study. *Procedia Comput. Sci*, 2020; 176(3): 582-591.
5. Benahmed A, M Mekhfioui, M Guennoun. FPGA based Hardware Co-Simulation Implementation for Real-Time Image Blind Separation using ICA Algorithms. *Int. J. Emerg. Technol. Adv. Eng.*2022; 12(9):75-8.
6. Hao J, Yang Y, Zhou Z, et al. Fetal Electrocardiogram Signal Extraction Based on Fast Independent Component Analysis and Singular Value Decomposition. *Sensor.* 2022; 22(5): 3705.
7. Alessandra Galli, Elisabetta Peri, Chiara Rabotti, et al. Automatic Optimization of Multichannel Electrode Configurations for Robust Fetal Heart Rate Detection by Blind Source Separation. *IEEE transactions on biomedical engineering*. 2023; 70(3): 443-452.
8. Jiménez González, A Castañeda Villa. Blind extraction of fetal and maternal components from the abdominal electrocardiogram: An ICA implementation for low-dimensional recordings. *Biomed Signal Process Control.* 2020; 58(1):101836.
9. V Vigneron, A Paraschiv Ionescu, A Azancot O, et al. Fetal electrocardiogram extraction based on non-stationary ICA and wavelet denoising: in *Proceedings of the Seventh International Symposium on Signal Processing and Its Applications*. 2003; 6(3): 69-72.
10. Braun F, Bonnier G, Rapin M, et al. Evaluation of a Wearable System for Fetal ECG Monitoring Using Cooperative Sensors: *Annu Int Conf IEEE Eng Med Biol Soc*. 2022; 7(2):31-45.
11. Mahfuzur Rahman, Bashir I Morshed. Resource-Constrained On-Chip AI Classifier for Beat-by-Beat Real-Time Arrhythmia Detection with an ECG Wearable System. *Edge AI for Biomedical Applications: Innovations in Sensing, Computing and Security*.Electronics 2025; 14(13):2654.
12. Shi X, Yamamoto K, Ohtsuki T, et al. Unsupervised Learning-Based Non-Invasive Fetal ECG Muti-Level Signal Quality Assessment. *Bioengineering* 2023; 10(1): 66.
13. Dash S S, Nath M K, Anbalagan T. Identification of FECG from AECG Recordings using ICA over *EMD*. Proceedings of *2023 International Conference on Medical Imaging and Computer-Aided Diagnosis.* 2023; 1(1):9-10.
14. Dash S S, Nath M K. A Novel Approach for Detecting Fetal QRS and Estimating Fetal Heart Rate from Abdominal ECG Using EMD and Wavelet Decomposition. Circuits *Syst Signal Process.* 2025; 1(1):10-19.
15. Mekhfioui M, Benahmed A, Chebak A, et al .The Development and Implementation of Innovative Blind Source Separation Techniques

for Real-Time Extraction and Analysis of Fetal and Maternal Electrocardiogram Signals. *Bioengineering*. 2024; 11(3): 512-521.

16. Nguetsop Hermann Beaumont, Gamom Ngounou, Jean Mbihi. Blind separation of three signals using Matlab/Simulink software and Arduino Due board. Available online www.ejaet.com, *European Journal of Advances in Engineering and Technology*. 2024; 11(7):1-11.
17. Mohcin Mekhfioui, Rachid Elgouri, Amal Satif, et al. Comparative Approach of Blind Source Separation with Arduino Due and TMS320C6713. *www.warse.org/IJETER Research.* 2020; 8(3):09-12.
18. Mohcin Mekhfioui, Rachid Elgouri, Amal Satif, et al. Real-Time Implementation Of A New Efficient Algorithm For Source Separation Using Matlab & Arduino Due. *Ijeter.* 2020; 04(2):1-4.
19. Rumana Islam, Mohammed Tarique. Blind Source Separation of Fetal ECG Using Fast Independent Component Analysis and Principle Component Analysis. *International journal of scientific & technology research*.2020; 9(11): 112-117.
20. Soumitra Das. Wearable Fetus Monitoring: An IoMT. *Journal of Scientific Research Institute of Science, Banaras Hindu University, Varanasi, India. Approach*. 2020; 64(2): 71-84.
21. Frank Martínez Suárez, José Alberto García Limón, Dalila Rivera-Córdova. Long-Term Continuous Ambulatory ECG Monitor with Beat-to-Beat Heart Rate Measurement in Real Time using ESP32. 2022 19th International Conference on Electrical Engineering, *Computing Science and Automatic Control (CCE)*. Mexico City; 2022; 1(1): 9-11.
22. Mhajna M, Schwartz N, Levit Rosen L, et al. Wireless remote solution for home fetal and maternal heart rate monitoring. *Am J Obstet Gynecol MFM.* 2020; 2 (2):100101.
23. L Qiao, S Hu, B Xiao, et al. A Dual Self-Calibrating Framework for Noninvasive Fetal ECG R-Peak Detection. *IEEE Internet of Things Journal*.2023; 10 (18): 16579-16593.
24. A J D Krupa, S Dhanalakshmi, R Kumar. Joint time-frequency analysis and non-linear estimation for fetal ECG extraction. *Biomedical Signal Processing and Control*. 2022; 75:103569.
25. D Edwin Dhas, M Suchetha. Extraction of Fetal ECG from Abdominal and Thorax ECG Using a Non-Causal Adaptive Filter Architecture. *IEEE Transactions on Biomedical Circuits and Systems*. 2022; 16(5): 981-990.
26. Nguetsop Hermann Beaumont, Gamom Ngounou, Jean Mbihi, et al. Low Cost Baby Incubator With Temperature, Humidity Controlling And Beat-To-Beat Fetal Heart Rate Analysis Using Gsm Technology And ESP 32 Board. *AJBR*.2025; 28(3):704–724.
27. Khizra Saleem, Fariha Ashfaq. Smart Health Monitoring System for Pregnant Women of Rural Regions. *Journal of Computers and Intelligent Systems.* 2023*;*1(1) : 42–58.
28. Danilo Pani, Eleonora Sulas, Monicaz Urru, et al. NiNFEA: Non-Invasive Multimodal Foetal ECG-Doppler Dataset for Antenatal Cardiology Research.2020; 2(1): 45-51.
29. Jabed Rana Ridoy, Shanjana Shaznin, Chaluvaraju P P. IOT Based Low Cost ECG Monitoring System .*International Journal of Research Publication and Reviews*. 2023; 1: 2582-7421.
30. Jess Mclntosh, Mike Fraser, Paul Worgan, et al .DeskWave: Desktop interactions using low-cost icrowave Doppler arrays. *Proceedings of the 2017 CHI conference extended abstracts on human factors in computing systems*.2017; 17(4):1885-1892.
31. Amrutha Bhaskaran, Manish Arora. Evaluation of cyclic repetition frequency based algorithm for fetal heart rate extraction from fetal phonocardiography -Time QRS Detection Algorithm. *IEEE Trans. Biomed. Eng. BME*.2023; 32(3): 230-236.
32. PAN J, TOMPKINS W J. A Real-Time QRS Detection Algorithm. IEEE *Trans. Biomed.* BME.1985; 11(8): 21-36.
33. Behar Joachim, Andreotti Fernando, Zaunseder Sebastian, et al. An ECG model for simulating maternal-foetal activity mixtures on abdominal ECG recordings. *Physiol. Meas*. 2014; 35(2):1537–1550.
34. Andreotti F, Behar J, Zaunseder S, et al. An Open-Source Framework for Stress-Testing Non-Invasive Foetal ECG Extraction Algorithms. *Physiol Meas* .2016; 5(4):627–648.
35. Rowan SP, Lilly CL, Claydon EA, et al. Monitoring one heart to help two: Heart rate variability and resting heart rate using wearable technology in active women across the perinatal period. *BMC Pregnancy Childbirth*. 2022; 22(1):887-895.
36. Steve Ulriche Otam, E R Gamom Ngounou, Jean Mbihi, et al. Conception et Co-Simulation sur Cible FPGA d'un Système d'Acquisition du Signal ECG par Modulation en Rapport Cyclique et Filtrage Dérivateur. *International Journal of Innovation and Applied Studies*.2021 ; 31(3) :735-807.
37. I Voicu, J Girault, C Roussel, et al. Robust Estimation of Fetal Heart Rate from US Doppler Signals: P. Procedia (Ed.), *Proc. of the Int. Congress on Ultrasonic*, *Physics Procedia.* 2010;

3(4): 691–699.
38. Thomas M. Vollbrecht, MD. Fetal Cardiac MRI Using Doppler US Gating: Emerging Technology and Clinical Implications Radiology. *Cardiothoracic Imaging.* 2024; 6(2):230182.
39. Bekar A, N R Ong, MHA Aziz, et Al. Research on the seam performance of waterproof clothing based on continuous ultrasonic welding technology.*International journal of clothing science and technology*.2016;28(2):64-71.
40. Sarah jiang, perisa Ashar, MD Mobashir, et Al. Demographic reporting in biosignal datasets: a comprehensive analusis of the physionet open access database.*The digital health*.2024; 6(11):871-878.
41. Yáñez R, González-Camarena R, Berg K, et al. Comparison of Fetal Heart Rate Variability by Symbolic Dynamics at the Third Trimester of Pregnancy and Low-Risk Parturition. *Heliyon.* 2020 ; 6(4) : 03485.
42. Choodamani Bhattarai, Siddhartha Kumar Yadav, Subash Koirala. IoT Based ECG Using AD8232 and ESP3. *Biomedical Engineering Research*, *Nepal Journal of Science and Technology*. 2023: 2382-5359.
43. K Sri Vidya, P Rajesh Kumar, I Krishna et AL Continuous Portable Fetal Heart Rate Monitoring Device. Dogo Rangsang Research Journal*; UGC Care Group I Journal.*2022; 12(09): 2347-7180.
44. Mohamad Nur Aiman Jam, Lilywati Bakar, Zurina Abdul Wahab. Heart Rate Monitoring Robot by Using Arduino and NodeMCU ESP8266. *Progress in Engineering Application and Technology.* 2022; 3(2): 363-372.
45. Ekejiuba C O, Akingbade K F, Apena W O, et al. Development of a maternal health monitoring device with optimized battery usage for vital signs capturing in pregnancy. *Advance Journal of Science, Engineering and Technology Adv.*2024*;* 34(3): 9.
46. L Qiao, S Hu, B Xiao, et al. A Dual Self-Calibrating Framework for Noninvasive Fetal ECG R Peak Detection. *IEEE Internet of Things Journal*. 2023.10(18):16579-16593.
47. Negar Tavassolian, Arash Shokouhmand. Fetal Electrocardiogram Extraction Using Dual-Path Source Separation of Single-Channel Non-Invasive Abdominal Recordings. *IEEE TRANSACTIONS ON BIOMEDICAL ENGINEERING*. 2023.70(1): 283.
48. Sajad Farrokhi, Waltenegus Dargie, Christian Poellabauer. Reliable peak detection and feature extraction for wireless electrocardiograms. *Computers in Biology and Medicine*. 2025; 185(5): 109478.
49. Li X, Wan J, Peng X. Review of Non-Invasive Fetal Electrocardiography Monitoring Techniques. *Sensors.* 2025; 25(6): 1412-1419.
50. Priyanka T, Bidhya R, Anjali C, et al. IOT Based Health Monitoring System using Arduino Uno. International Advanced Research Journal in Science*, Engineering and Technology.*2021*;* 10(6):257-260.